Markov, fractal, diffusion, and related models of ion channel gating

A comparison with experimental data from two ion channels

M. S. P. Sansom,* F. G. Ball,‡ C. J. Kerry,* R. McGee,§ R. L. Ramsey,* and P. N. R. Usherwood*
Departments of Zoology* and Mathematics,‡ University of Nottingham, University Park, Nottingham, NG7 2RD, United Kingdom; and §Department of Pharmacology, Medical College of Ohio, Toledo, Ohio 43699

ABSTRACT The gating kinetics of single-ion channels are generally modeled in terms of Markov processes with relatively small numbers of channel states. More recently, fractal (Liebovitch et al. 1987. *Math. Biosci.* 84:37–68) and diffusion (Millhauser et al. 1988. *Proc. Natl. Acad. Sci. USA.* 85:1502–1507) models of channel gating have been proposed. These models propose the existence of many similar conformational substates of the channel protein, all of which contribute to the observed gating kinetics. It is important to determine whether or not Markov models provide the most accurate description of channel kinetics if progress is to be made in understanding the molecular events of channel gating. In this study six alternative classes of gating model are tested against experimental single-channel data. The single-channel data employed are from (*a*) delayed rectifier K^+ channels of NG108-15 cells and (*b*) locust muscle glutamate receptor channels. The models tested are (*a*) Markov, (*b*) fractal, (*c*) one-dimensional diffusion, (*d*) three-dimensional diffusion, (*e*) stretched exponential, and (*f*) expo-exponential. The models are compared by fitting the predicted distributions of channel open and closed times to those observed experimentally. The models are ranked in order of goodness-of-fit using a bootstrap resampling procedure. The results suggest that Markov models provide a markedly better description of the observed open and closed time distributions for both types of channel. This provides justification for the continued use of Markov models to explore channel gating mechanisms.

INTRODUCTION

Ion channels are transmembrane proteins that form ion-selective pores in lipid bilayer membranes. The opening and closing of these pores may be observed using patch clamp recording (Hamill et al., 1981). The theory of stochastic processes (Cox and Miller, 1965) enables one to relate the apparently random opening and closing of a channel to its underlying gating mechanism. Description of the gating mechanisms of ion channels provides one with important clues about the molecular processes whereby channel gating is controlled either by transmembrane voltage, or by binding of neurotransmitters to receptor sites.

Hitherto ion channel gating mechanisms have generally been modeled in terms of Markov processes with relatively small numbers of open and closed states of the channel (Colquhoun and Hawkes, 1981, 1982; Horn, 1984). The essence of Markov (M) models is that, for any single step in the gating mechanism, the transition probability (i.e., the microscopic equivalent of the rate constant) is time independent.

Considerable progress has been made, both theoretically and experimentally, in interpretation of channel gating kinetics in terms of such models. Early studies employed relatively simple models with, for example, a single, open state and two closed states of the channel. However, in several systems, the numbers of open and of closed states (N_o and N_c, respectively) have turned out to be somewhat larger. For example, Kerry et al. (1987, 1988; also see Ashford et al., 1984) have shown that at least four open states and four closed states are required to explain the gating kinetics of the quisqualate-sensitive glutamate receptor channel (qGluR) of locust muscle. Likewise, McManus and Magleby (1988) have interpreted the kinetics of Ca^{2+}-activated K^+ channels in terms of three or four open states and six to eight closed states, and Blatz and Magleby (1986a, 1989) have interpreted the gating of the fast Cl^- channel of rat skeletal muscle in terms of a model with five closed states and two open states.

More recently, there have been several suggestions that channel gating mechanisms might not be adequately described by simple Markov models. Alternative models proposed have the common feature of stressing that proteins may exist in many conformational substates (Frauenfelder et al., 1988), with each substate contributing to the observed channel gating kinetics. Liebovitch and colleagues (Liebovitch et al., 1987*a*, *b*; Liebovitch and Sullivan, 1987, Liebovitch, 1989*a*, *b*) have investigated fractal (F) models of ion channel gating, as have French and Stockbridge (1988). McManus et al. (1988, 1989) and Korn and Horn (1988; also Horn and Korn, 1989) have questioned the validity of such models.

Millhauser et al. (1988*a*, *b*) have suggested that diffusion (D) models may provide a better explanation of channel kinetics than M models. Although, strictly speaking, D models are still Markov processes, D models differ from the M models described above with respect to the much larger numbers of approximately equivalent channel states that they contain. Millhauser et al. (1988*a*, *b*) have focused on one-dimensional (D_1) models in which, for example, there may be a linear array of several hundred closed states, only one (or a few) of which is directly linked to the open state(s) of the channel. Lauger (1988) has investigated a similar model (D_3) in which the many equivalent closed states form a three-dimensional lattice.

In this paper we describe how we have tested M, F, and D models against experimental data recorded from two different channels, one receptor gated and one voltage gated. We also describe the testing of two other classes of model, one of which, to the best of our knowledge, has not previously been investigated in the context of ion channel gating kinetics. Given that our understanding of protein dynamics is incomplete, we feel that the only way to discriminate between alternative gating models is by careful statistical analysis of single channel data. To this end we have analyzed the gating kinetics of the two channels, the locust muscle qGluR (Kerry et al., 1987, 1988) and a delayed rectifier-type K^+ channel from NG108-15 cells (McGee et al., 1988), in terms of six different classes of gating models. A preliminary account of this work has appeared in abstract form (Ball et al., 1989).

METHODS

Experimental

Glutamate receptor channels were recorded using the megaohm patch clamp, as described by Kerry et al. (1987). A two-electrode voltage clamp was used to maintain the membrane potential at −110 mV, and the muscle was pretreated with concanavalin A to block desensitization. The gigaohm patch clamp method (Hamill et al., 1981) was used to record single, K^+ channel openings from cell attached patches of NG108-15 cells, as described by McGee et al. (1988). Channel openings were elicited in response to 20-s depolarizations to 0 mV, the membrane being hyperpolarized to −120 mV for 10 s before each depolarization. Single-channel currents were filtered at 5 kHz and stored either on FM tape at 30 in./s (qGluR) or on video tape using a PCM (Sony Corp., Tokyo, Japan) and VCR (K^+ channel).

Data reduction

Single-channel recordings were filtered at 3 kHz on playback, and analyzed using the dual-threshold crossing method as described by Kerry et al. (1987). The open and closed (dwell) times were written to disc. Data were subsequently processed to exclude all dwell times of duration less than t_{min} (Colquhoun and Sigworth, 1983) by combination of the two adjacent intervals with the intervening brief ($\leq t_{min}$) interval. The data reduction was carried out on a PDP 11/34 computer (Digital Equipment Corp., Maynard, MA). The files of dwell times were transferred to a model MC5500 computer (Masscomp, Westford, MA), which was used for all data analysis. The analysis programs were written in Fortran 77 and drew on the Numerical Algorithms Group library (Oxford, UK) of numerical subroutines.

Dwell time histograms

Dwell time histograms were constructed using exponential binning, as described by Kerry et al. (1988). Briefly, the minimum (t_{min}) and maximum (t_{max}) dwell times for a histogram were used to calculate the bin width ratio

$$g = (t_{max}/t_{min})^{1/m}, \tag{1}$$

where m is the number of bins. The ith bin is then defined by

$$t_{min}g^{i-1} \leq t < t_{min}g^{i} \tag{2}$$

and is of width

$$t_{min}(g^{i} - g^{i-1}) \tag{3}$$

and is centered about

$$t_i = t_{min}g^{i-1/2}. \tag{4}$$

Exponential binning of the data permits a wide range of dwell times (e.g., from 0.15 ms to 10 s for the K^+ channel data) to be incorporated in the same histogram. It is also of importance with respect to the fitting of dwell time distributions (see below). The dwell time histograms were displayed on log–log plots (McManus et al., 1987; Kerry et al., 1988). Normalization of the histograms to unit area was carred out to enable comparison of histograms from datasets of different total numbers of events.

Fitting dwell time distributions

General aspects of fitting dwell time probability density functions (PDFs) to observed distributions are described here. Details of the PDFs for different gating models are described in the following Theory section. Model PDFs were fitted to dwell time histograms using the maximum likelihood method (see e.g., Colquhoun and Sigworth, 1983; McManus et al., 1987). Let $f(t)$ represent the dwell time PDF to be fitted. Then the log-likelihood of observing a set of dwell times t_i, $i = 1, \ldots, n$ for a model with parameter vector θ is given by

$$L(\theta) = \log \prod_{i=1}^{n} f(t_i|\theta), \tag{5}$$

which can be rewritten (dropping the θ for convenience) as

$$L = \sum_{i=1}^{n} \log f(t_i). \tag{6}$$

To evaluate L in this manner would be rather computationally demanding for the datasets under consideration, where n is of the order of 10,000. Instead, a close approximation to L is obtained by considering the binned data (see e.g., Blatz and Magleby, 1986*b*), i.e., if there are m bins, with bin j containing y_j events, centered about t_j, the log-likelihood is given by

$$L = \sum_{j=1}^{m} y_j \log f(t_j). \tag{7}$$

Maximization of L with respect to the parameters θ than yields the "best" estimate of the model parameters $\hat{\theta}$. Maximization was carried out using a simplex algorithm (NAG subroutine E04CCF). Searching for the maximum was carried out on a transformed parameter space (ϕ) where the transformation $\phi = h(\theta)$ was defined for each model to prevent evaluation of L for physically meaningless parameter values. Details of the transformations used are given below.

Having estimated $\hat{\theta}$, fits to the distributions were checked by superimposition of the observed (f_{obs}) and calculated (f_{cal}) distributions. Cumulative errors were evaluated (McManus and Magleby, 1988) as defined by

$$E_j = \sum_{k=1}^{j} y_k(|f_{obs,k} - f_{cal,k}|)/f_{cal,k}, \quad (8)$$

where y_k is the number of events in bin k.

Discrimination between alternative models

The primary aim of this study was to discriminate between fits of alternative forms of PDF to the same observed dwell time distributions so as to select the model giving the best description of the data. To do this we used the Schwarz criterion (SC) (Schwarz, 1978; Landaw and DiStefano, 1984) as a measure of the goodness of fit of model to data. In the current context the SC is given by

$$SC = -\hat{L} + \tfrac{1}{2}N_{par} \ln M, \quad (9)$$

where $\hat{L}$ is the maximum log-likelihood, N_{par} is the number of free parameters in the model, and M is the number of observations. Thus $-\hat{L}$ is more negative the better the fit, and $\tfrac{1}{2}N_{par} \ln M$ is a positive penalty term which increases with the number of free parameters in the model. The SC is therefore closely related to the AIC (Akaike, 1974) employed by e.g., Horn (1987) to distinguish between alternative channel models, the difference being that the penaly term is larger in the SC. Ball and Sansom (1989) presented evidence suggesting that the SC leads to correct model selection more frequently than the AIC. If the SC's from fitting model X and model Y to the same data are SC_X and SC_Y, respectively, then we can define an SC predictor $P_{X/Y}$ such that

$$\begin{aligned} P_{X/Y} &= SC_Y - SC_X \\ &= (\hat{L}_Y - \hat{L}_X) + \tfrac{1}{2}(N_{par,Y} - N_{par,X}) \ln M. \end{aligned} \quad (10)$$

Thus, if model X describes the data better than model Y, $P_{X/Y}$ is positive; if both models describe the data equally well the predictor is zero; and if model Y gives the better description the predictor is negative.

It is clearly desirable to have some measure of how robust the SC ranking of models is to sampling variations in the dwell time dataset. To this end, we have employed the bootstrap resampling procedure of Efron (1981, 1982), which was first applied to channel data by Horn (1987). It should be noted that this procedure is based upon the assumption that the channel dwell times are independently and identically distributed. Although this is not strictly the case (successive dwell times may be correlated), it is unlikely to cause problems as models are fitted under the assumption of independent data values. To perform the bootstrapping, the original vector of dwell times is resampled, with replacement, to produce, e.g., 50 equivalent resampled datasets. Within each resampled dataset some original dwell times are unrepresented, some are represented once, some twice, and so on. The expected proportion of dwell times in the original dataset absent from the resampled dataset is approximately e^{-1} (Efron, 1982), e.g., of 10,000 dwell times, ~3,700 would be absent. Resampling was carried out independently for open and for closed times. Each of the resampled datasets was used to produce a binned dataset, which was then fitted with the PDFs for, e.g., model X and model Y. Thus, 50 values of $P_{X/Y}$ were generated. A histogram of these was constructed and fitted with a normal distribution. The mean and variance of the normal distribution were then used to estimate the probability that $P_{X/Y} > 0$, given the bootstrap resampling. In this manner one may obtain a "significance" level for the SC ranking of two different models fitted to a particular dataset.

THEORY

In this section we describe the different gating models, and outline the derivation of the corresponding PDFs. It is also necessary to take into account the effect of omission of dwell times less than t_{min} or greater than t_{max} on the agreement between observed distributions and fitted PDFs. Here we are not concerned with a full correction for event omission (see, e.g., Roux and Sauvé, 1985; Blatz and Magleby, 1986*b*; Ball and Sansom, 1988*a*, *b*, for accounts of such corrections for M models) but, rather, with scaling of the PDFs fitted such that the integral between t_{min} and t_{max} is equal to unity. This is the same scaling as has been applied to the dwell time histograms. If the unscaled PDF is $f(t)$, then let the corresponding cumulative distribution function be $F(t)$. The scaled PDF is given by

$$g(t) = \frac{f(t)}{\text{Prob}\,(t_{min} \le t < t_{max})} = \frac{f(t)}{F(t_{max}) - F(t_{min})}, \quad (11)$$

and it is this scaled PDF that is fitted to be observed distribution using the maximum likelihood procedure outlined above. For convenience we will, in the following sections, discuss the different models in terms of the closed time distributions. It should be understood that exactly parallel arguments can be applied to the open time distributions.

Markov (M) models

The theoretical background to this class of models has been described in detail by several authors (Colquhoun and Hawkes, 1981, 1982; Horn, 1984). The basic assumptions are (*a*) a small number of distinct channel states; and (*b*) time-invariant transition rates. If there are N_c closed states, the closed time PDF is the sum of at most N_c exponential decays

$$f(t) = \sum_{i=1}^{N_c} (\alpha_i/\tau_i) \exp(-t/\tau_i), \quad (12)$$

where the parameters α_i and τ_i may be derived from the closed-state transition matrix (Q_{cc}) for the gating mechanism, as described by Colquhoun and Hawkes (1982).

The scaled PDF is

$$g(t) = \frac{\sum_{i=1}^{N_c} (\alpha_i/\tau_i) \exp(-t/\tau_i)}{\sum_{i=1}^{N_c} \alpha_i [\exp(-t_{min}/\tau_i) - \exp(-t_{max}/\tau_i)]}, \quad (13)$$

and this is used to evaluate the log-likelihood via Eq. 7. The transformation applied to the parameter space is

$$\phi_{2i-1} = (\alpha_i^{-1} - 1)^{1/2}$$
$$\phi_{2i} = \log \tau_i, \quad (14)$$

where $i = 1, \ldots, N_c$ and with the additional constraint that $\Sigma_{i=1}^{N_c} \alpha_i = 1$. This ensures that all α_i values range between 0 and 1 and that all τ_i values are positive.

Fractal (F) models

These have been explored in some detail by Liebovitch and coworkers (Liebovitch et al., 1987*a*, *b*; Liebovitch, 1989*a*). The basic assumption is that once the channel closes, the reopening rate is dependent on the time spent closed, such that the rate of reopening declines as the closed time increases. Thus the Markov condition of constant transition rates is broken. If the rate of reopening of the channel is $k(t)$:

$$C \xrightarrow{k(t)} O,$$

then the time dependence is given by

$$k(t) = At^{1-D},$$

where A is the kinetic setpoint and D is the fractal dimension of the model, falling in the range $1 \leq D < 2$. Thus, the value of D determines the extent to which the PDF is stretched over a wider range of closed times than would be the case for a monoexponential PDF. Note that $D = 1$ yields $k(t) \equiv A$, i.e., the simplest M model, with a single closed state of mean lifetime A^{-1}. The PDF for the F model is

$$f(t) = At^{1-D} \exp[-At^{2-D}/(2 - D)]. \quad (16)$$

For $D = 1$ this reduces to a single exponential with time constant $1/A$. As D increases the PDF is stretched towards higher dwell times. The corresponding scaled PDF is

$$g(t) = \frac{At^{1-D} \exp[-At^{2-D}/(2 - D)]}{\exp[-At_{min}^{2-D}/(2 - D)] - \exp[-At_{max}^{2-D}/(2 - D)]} \quad (17)$$

The transformation applied to the parameters during maximization of L is

$$\phi_1 = \log A$$
$$\phi_2 = \left[\frac{D - 1}{2 - D}\right]^{1/2}, \quad (18)$$

thus ensuring that A is positive and that D falls in the allowed range.

Diffusion (D_1 and D_3) models

In these models, once the channel has closed, it is viewed as diffusing away from the gateway state (that from which reopening may occur) via transitions among a large number of equivalent closed states. We have examined two types of diffusion model: the one-dimensional (D_1) model of Millhauser et al. (1988*a*, *b*) and the three-dimensional (D_3) model of Lauger (1988).

The D_1 model consists of a linear array of closed states

$$C_{N_c} \underset{\lambda}{\overset{\lambda}{\rightleftharpoons}} C_{N_c-1} \underset{\lambda}{\overset{\lambda}{\rightleftharpoons}} \cdots\cdots \underset{\lambda}{\overset{\lambda}{\rightleftharpoons}} C_2 \underset{\lambda}{\overset{\lambda}{\rightleftharpoons}} C_1 \xrightarrow{\beta} O,$$

where β is the rate of opening from the gateway state C_1, and where λ is the interconversion rate between any pair of closed states. N_c is large, e.g., ~50 or more. Strictly speaking this is still a Markov process, albeit with a large state space, so it is straightforward to set up the closed-state transition matrix Q_{cc} (see Appendix 1) and hence to evaluate α_i and τ_i ($i = 1, \ldots, N_c \geq 50$) for substitution in Eqs. 12 and 13. Of course, there are in this case only two free parameters, β and λ, which are transformed during maximization of L using

$$\phi_1 = \log \beta$$
$$\phi_2 = \log \lambda \quad (19)$$

to ensure positive values for both rate constants.

The D_3 model is similar, with β and λ defined as before, but with the closed states arranged on three-dimensional lattice (Fig. 1). We examined the simplest version of this model, with $N_c = 3 \times 3 \times 3 = 27$. By exploiting the symmetry properties of the transition matrix Q_{cc} it is possible to reduce this to an equivalent model with $N_c =$ nine closed states (Appendix 2). The α_i and τ_i values are evaluated as before. The same parameter transformations are employed as for the D_1 model.

Williams-Watts (W) model

This class of model has been used to explain nonexponential relaxation phenomena in complex condensed matter systems, e.g., dielectric relaxation in polymers and glasses

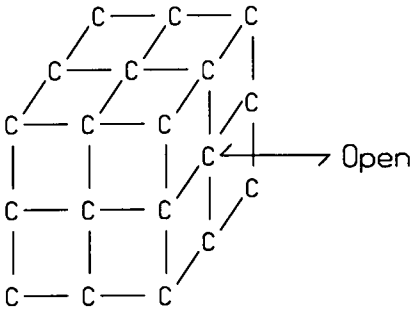

FIGURE 1 Diagram of the three-dimensional diffusion model (D_3) (Lauger, 1988) in its simplest form, with 27 energetically equivalent closed states. The closed states are arranged in a 3 × 3 × 3 lattice, and the (↔ closed) transition rate is λ. There is a single, closed gateway state from which the channel can open, with opening rate β.

(Shlesinger and Montroll, 1984; Klafter and Blumen, 1985; Klafter and Shlesinger, 1986). As discussed by Frauenfelder et al. (1988) glasses are thought to have similar conformational substate properties to proteins, and so it seemed appropriate to investigate W models as a possible explanation of the relaxation of a channel after closing. Klafter and Shlesinger (1986) have shown that several different types of underlying molecular processes give rise to the W model, which is characterized by stretched exponential relaxation kinetics. In terms of a channel dwell time PDF this may be written as

$$f(t) = \frac{\beta}{\tau\Gamma(1/\beta)} \exp\ [-(t/\tau)^{\beta}], \qquad (20)$$

where $0 < \beta \leq 1$ and where Γ is the gamma function. Note that if $\beta = 1$ then this reduces to a simple monoexponential PDF, which is stretched to cover a greater range of t values as β decreases. The scaled PDF is

$$g(t) = \frac{f(t)}{F(t_{max}) - F(t_{min})}, \qquad (21)$$

where

$$F(t) = \int_0^t \frac{\beta}{\tau\Gamma(1/\beta)} \exp\ [-(t/\tau)^{\beta}]\, dt, \qquad (22)$$

this integral (an incomplete gamma function)being evaluated numerically. The parameter transformation adopted during maximization is

$$\phi_1 = \log \tau$$

$$\phi_2 = (1/\beta - 1)^{1/2} \qquad (23)$$

ensuring that τ remains positive and β within the range specified above.

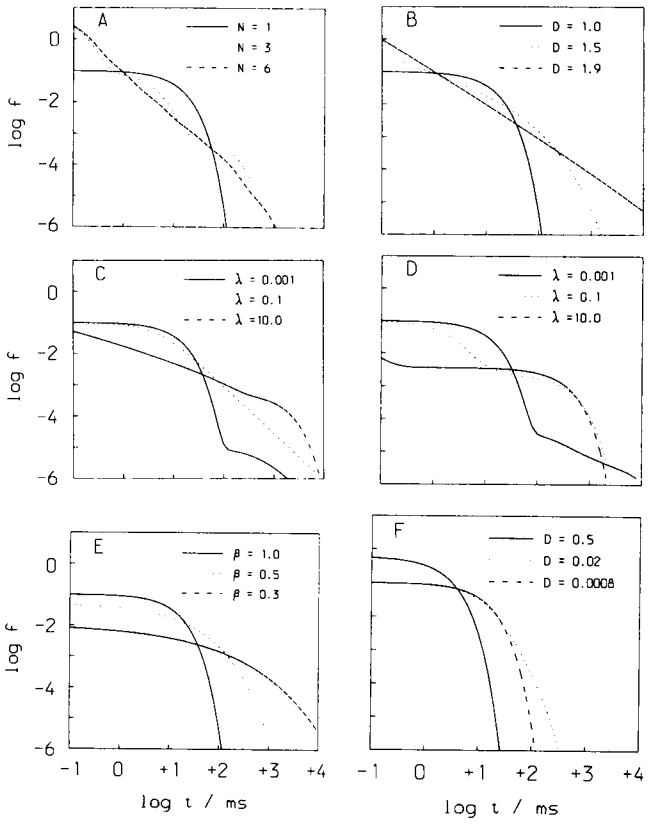

FIGURE 2 Calculated PDFs for the six different classes of gating model. In each case, the scaled PDFs (t_{min} = 0.1 ms, t_{max} = 10,000 ms) are displayed on a log–log plot. (*A*) PDFs for three Markov (M) models, with $N = 1$ ($\alpha = 1.0$, $\tau = 10$ ms, *solid line*); $N = 3$ ($\alpha_1 = 0.6$, $\tau_1 = 0.1$ ms; $\alpha_2 = 0.3$ $\tau_2 = 3.0$ ms; $\alpha_3 = 0.1$, $\tau_3 = 100$ ms, *dotted line*); and $N = 6$ ($\alpha_1 = 0.6$, $\tau_1 = 0.1$ ms; $\alpha_2 = 0.2$, $\tau_2 = 0.5$ ms; $\alpha_3 = 0.1$, $\tau_3 = 2.5$ ms; $\alpha_4 = 0.05$, $\tau_4 = 12.5$ ms; $\alpha_5 = 0.04$, $\tau_5 = 62.5$ ms; $\alpha_6 = 0.01$, $\tau_6 = 312.5$ ms, *dashed line*). (*B*) PDFs for three fractal (F) models, with $A = 0.1$ ms^{D-1} in each case. *Solid line* $D = 1.0$; *dotted line* $D = 1.5$; and *dashed line* $D = 1.9$. (*C*) PDFs for one-dimensional diffusion (D_1) models, with $N = 100$ and $\beta = 0.1$ ms^{-1} in each case. *Solid line* $\lambda = 0.001$ ms^{-1}; *dotted line* $\lambda = 0.1$ ms^{-1}; and *dashed line* $\lambda = 10.0$ ms^{-1}. (*D*) PDFs for three-dimensional diffusion (D_3) models, with $N = 3 \times 3 \times 3 = 27$ and $\beta = 0.1$ ms^{-1} in each case. *Solid line* $\lambda = 0.001$ ms^{-1}; *dotted line* $\lambda = 0.1$ ms^{-1}; and *dashed line* $\lambda = 10.0$ ms^{-1}. (*E*) PDFs for Williams-Watts (W) models, with $\tau = 10$ ms in each case. *Solid line* $\beta = 1.0$; *dotted line* $\beta = 0.5$; and *dashed line* $\beta = 0.3$. (*F*) PDFs for expo-exponential (E) models, with $A = 0.1$ ms^{-1} in each case. *Solid line* $D = 0.5$ ms^{-1}; *dotted line* $D = 0.02$ ms^{-1}; and *dashed line* $D = 0.0008$ ms^{-1}.

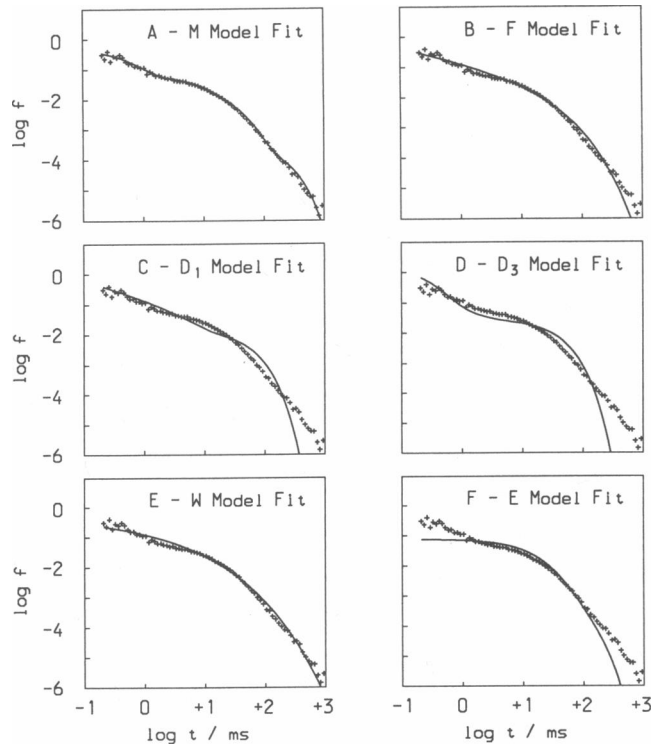

FIGURE 3 Closed time distribution for qGluR. In each graph the observed distribution is shown as points with the fitted PDF as the superimposed curve. The parameters for the fitted curves are in Table 1. The fits for the six different classes of model are shown. (*A*) Markov; (*B*) fractal; (*C*) one-dimensional diffusion; (*D*) three-dimensional diffusion; (*E*) Williams-Watts; and (*F*) expo-exponential.

Expo-exponential (E) model

This model was originally proposed by Easton (1978) as an explanation of the macroscopic kinetics of the Na^+ and of K^+ currents of squid giant axon. More recently it has been discussed in the context of single-channel gating kinetics by Horn (1987). It holds some similarities to the F model in that the reopening rate of the closed channel is time dependent

$$C \xrightarrow{k(t)} O$$

but in the E model the opening rate decreases exponentially with increasing time

$$k(t) = A \exp(-Dt). \tag{24}$$

(The A and D nomenclature is used to highlight the relationship to the F model.) Horn (1987) has suggested that this may be interpreted in terms of the rate of reopening of the channel being proportional to the level of a diffusible substance, the concentration of which decreases exponentially subsequent to closing. In this interpretation D is the rate constant for the decline of this substance, and A is the reopening rate immediately after closing. The PDF for the E model is therefore

$$f(t) = A \exp(-Dt) \exp[A(\exp(-Dt) - 1)/D], \tag{25}$$

which upon scaling for event omission yields:

$$g(t) = \frac{A \exp(-Dt) \exp[A(\exp(-Dt) - 1)/D]}{\exp[A(\exp(-Dt_{min}) - 1)/D] - \exp[A(\exp(-Dt_{max}) - 1)/D]} \tag{26}$$

The parameters are transformed during maximization of L so that both A and D remain positive using

$$\phi_1 = \log A$$

$$\phi_2 = \log D \tag{27}$$

Comparison of predicted PDFs

Fig. 2 illustrates the shapes of the PDFs predicted by the different classes of model, as seen on log–log scales. For

TABLE 1 GluR closed time PDFs

Model	Parameters		*SC*	Rank	P_{obs}
M	$\alpha_1 = 0.186$ $\alpha_2 = 0.319$ $\alpha_3 = 0.444$ $\alpha_4 = 0.051$	$\tau_1 = 0.453$ ms $\tau_2 = 7.40$ ms $\tau_3 = 23.5$ ms $\tau_4 = 146$ ms	1.864×10^5	1	0.921
F	$A = 0.147$ ms^{D-1}	$D = 1.46$	1.871×10^5	2	0.894
D_1	$\beta = 4.95$ ms^{-1}	$\lambda = 198$ ms^{-1}	1.905×10^5	4	0.852
D_3	$\beta = 1.47$ ms^{-1}	$\lambda = 0.710$ ms^{-1}	1.933×10^5	6	0.812
W	$\tau = 0.272$ ms	$\beta = 0.323$	1.873×10^5	3	0.945
E	$A = 0.0753$ ms^{-1}	$D = 0.0166$ ms^{-1}	1.917×10^5	5	0.974

The model parameters and the *SC* are defined in the text. P_{obs} is the probability of observation of a closing between the minimum and maximum dwell time durations (see Eq. 11).

each model, it is possible to change the model parameters such that a single-exponential decay is stretched out to cover a much wider range of dwell times. Thus, in qualitative terms each model is capable of explaining the wide ranges of dwell times observed experimentally. So, it is the more detailed differences in the shapes of the resultant PDFs that allow us to discriminate between the models in terms of how accurately they account for the observed dwell time distributions.

RESULTS

Locust muscle qGluR

Open and closed time distributions derived from qGluR recordings made in the presence of 0.1 mM glutamate were analyzed. The recordings were from six separate membrane patches. After imposition of a minimum dwell time of t_{min} = 0.2 ms, the dataset consisted of 48,814 openings. For the open time distribution t_{max} = 100 ms, for the closed time distribution t_{max} = 1,000 ms.

Closed time distribution

Channel-closed times range from 0.2 ms to 1 s. The observed distribution of closed times (Fig. 3) shows distinct shoulders at ~0.5, 30, and 300 ms, as would be expected if an M model explains the gating kinetics.

As described by Kerry et al. (1988) the "best" fit to the closed time distribution for an M model has N_c = 4 exponentially decaying components (Fig. 3 *A*) The time constants (Table 1) are relatively well separated, hence the distinct shoulders in the fitted curve, which correspond well with those in the observed distribution. The model agrees excellently with the data for both the long- and brief-duration extremes of the distribution.

The F model also gives a reasonable fit to the data (Fig. 3 *B*), but the frequency of long closings is underpredicted. The fractal dimension, D = 1.46, is midway between the two limits, thus stretching the predicted PDF out over the range of qGluR closed times. The lower value of P_{obs} (the probability of a closed time duration falling between t_{min} and t_{max}) than that for the M model (Table 1), reflects the greater frequency of omission of brief closings for the F model fit.

The two diffusion models yielded less convincing fits to the data (Fig. 3 *C* and *D*). Both considerably underestimated the frequency of long duration closings. The fit for the D_1 model had $\lambda \gg \beta$. This corresponds to the situation in which, once closed, the channel rapidly "diffuses" amongst the closed states before (eventually) reopening. This corresponds to a case explored in detail by Millhauser et al. (1988*a*) who predicted that under such conditions, the PDF would be approximately proportional to $t^{-1/2}$ for dwell times of intermediate duration. The log–log slope at t = 0.2 ms for the PDF is ~ −0.6, which is in agreement with this prediction. The log–log slope of the observed distribution for longer duration closings (30–

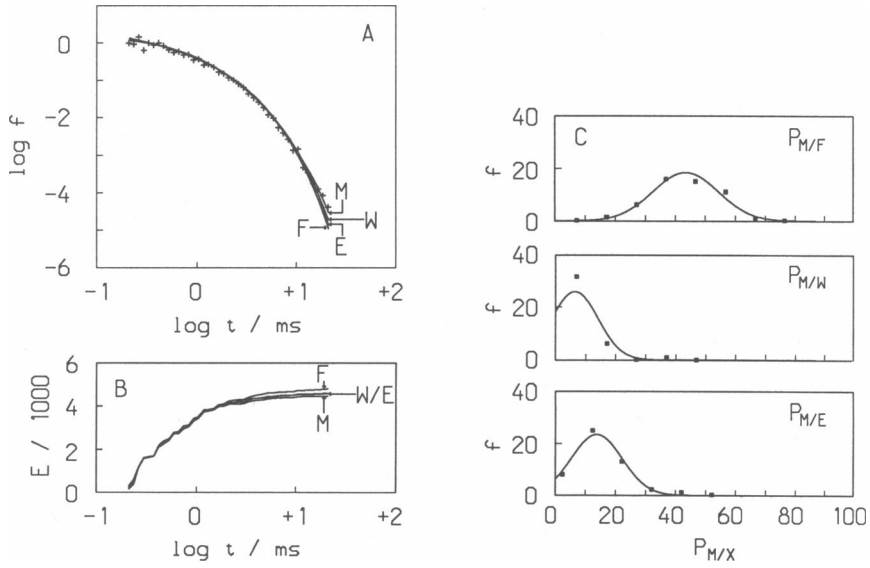

FIGURE 4 Open time distribution for qGluR. (*A*) The observed distribution is shown with the PDFs for the four best-fitting models (M, F, W, and E). The parameters for the curves are given in Table 2. (*B*) The corresponding cumulative error curves. (*C*) The distributions of SC predictors for the F, W, and E models compared with the M model (the *solid squares* represent the heights of the bars of the predictor histograms), along with fitted normal distributions (see Table 3).

TABLE 2 GluR open time PDFs

Model	Parameters		*SC*	Rank	P_{obs}
M	$\alpha_1 = 0.402$ $\alpha_2 = 0.523$ $\alpha_3 = 0.075$	$\tau_1 = 0.440$ ms $\tau_2 = 1.26$ ms $\tau_3 = 3.01$ ms	5.250×10^4	1	0.771
F	$A = 0.873$ ms^{D-1}	$D = 1.28$	5.255×10^4	3	0.680
D_1	$\beta = 0.909$ ms^{-1}	$\lambda = 0.0131$ ms^{-1}	5.388×10^4	4	0.827
D_3	$\beta = 0.887$ ms^{-1}	$\lambda = 0.00427$ ms^{-1}	5.390×10^4	5	0.819
W	$\tau = 0.304$ ms	$\beta = 0.585$	5.251×10^4	2	0.737
E	$A = 1.20$ ms^{-1}	$D = 0.417$ ms^{-1}	5.251×10^4	2	0.738

1,000 ms) is ~ -2.5, which is inconsistent with the predictions of Millhauser et al. (1988*a*). This discrepancy presumably underlies the failure of the D_1 model to account for the long closings.

The D_3 model also yields a poor fit to the long closings (Fig. 3 *D*). For this fit $\beta \approx \lambda$, i.e., immediately after closing, the channel has approximately equal probabilities of reopening and of "diffusing" into the closed-state lattice.

Turning to the W model (Fig. 3 *E*), this adequately accounts for both brief and long closings, but fails to fit the shoulders on the distribution. The value adopted by $\beta = 0.323$ sufficiently stretches the exponential distribution to cover the range of closed times.

Finally, the E model fit (Fig. 3 *F*) is also stretched across the range of closed times, by a combination of low values for both *A* and for *D*. However, the observed frequencies of both brief and long closings are greatly underpredicted.

The six different fits to the qGluR closed time distribution may be ranked by their *SC*'s. This reveals the M model to be the best fit (rank 1), with the F model ranked second. The results of bootstrap analysis of the model rankings are discussed below. Examination of the *SC* values for the M and F fits (Table 1) reveals a considerable difference, suggesting that the M model gives a significantly better fit. Given the pronounced shoulders in the observed distribution, this is not altogether surprising.

Open time distribution

The observed qGluR open time distribution is illustrated in Fig. 4 *A*. It is stretched over a greater time range than for a single exponential distribution (compare with Fig. 2 *A*), but there are no distinct shoulders. The open times range from 0.2 to ~30 ms in duration.

The M model fit has $N_o = 3$ components, as originally noted by Kerry et al. (1987). The time constants are relatively close together (Table 2), which is consistent with the absence of pronounced shoulders in the distribution. The M model PDF fits the data well, for both long and for brief openings.

Three other models (F, W, and E) also give reasonable fits to the data (Fig. 4 *A*), although all three predict the frequency of long openings less accurately than does the M model. Examination of the cumulative error curves (Fig. 4 *B*) suggests that the M model gives the best fit, with W and E next best, and then the F model. On the basis of the *SC*'s one would adopt the same ranking (Table 2). The W model fit has $\beta = 0.585$, thus stretching the exponential, but to a lesser extent than for the closed

TABLE 3 Predictor ratios from boostrap analysis

Dataset	Predictor ratio (±SD)				
	$\bar{P}_{M/F}$	$\bar{P}_{M/D_1}$	$\bar{P}_{M/D_3}$	$\bar{P}_{M/W}$	$\bar{P}_{M/E}$
GluR, closed times	742 (±53)	4070 (±140)	6860 (±220)	963 (±61)	5300 (±130)
GluR, open times	43.2 (±10.8)	1500 (±50)	1530 (±50)	6.2 (±7.7)	13.5 (±8.6)
K^+ channel, closed times	308* (±30)	114 (±16)	2220‡ (±100)	2170 (±130)	18700 (±500)
K^+ channel, open times	284 (±34)	1770 (±80)	187 (±21)	491 (±33)	1170 (±210)

50 bootstrap resampled datasets were used in all cases except two: * where 39 and ‡ where 41 were used respectively.

times. The value of $D = 1.28$ for the F model again gives a small deviation from a single-exponential PDF.

The two diffusion models (D_1 and D_3) both yield poor fits (Table 2) to the data. In both cases $\lambda \ll \beta$ which means that the open states other than the gateway state are rarely sampled, and so the PDFs are approximately equivalent to single exponential decays. The D_1 fit was for $N_o = 50$ open states. We also fitted a D_1 model with 100 open states, but no significant improvement was obtained.

To distinguish between the M, F, W, and E model fits to the qGluR open time data, the bootstrapping procedure was employed, the results of this analysis being presented in Fig. 4 *C*, and in Table 3. The distributions of $P_{M/X}$ in Fig. 4 *C* are all centered to the right of zero, which is consistent with the M model providing the best description of the data. By fitting normal curves to the predictor distributions, one can estimate the probability, given the bootstrap resampling, that the M model provides a better description of the data. For the F model, $\bar{P}_{M/F} = 43.2$, with probability $1 - 3.2 \times 10^{-5}$. For the W model, $\bar{P}_{M/W} = 6.2$, with probability 0.79. Finally, for the E model, $\bar{P}_{M/E} = 13.5$, and the probability is 0.95. Consequently, we have ~80% "confidence" that the M model fits the data better than its nearest rival. Thus, use of the bootstrap resampling distribution of the *SC* predictor allows a decision to be made, even in the situation where the difference in the fits of two models is small.

NG108-15 K^+ channels

Delayed rectifier-type K^+ channel openings were recorded in response to a 20-s membrane depolarization. All events other than the initial and the final closed times are included in the dataset, which derives from two membrane patches. After setting $t_{min} = 0.15$ ms, the total number of openings is 14,642. For the closed times, $t_{max} = 10$ s; for the open times $t_{max} = 1000$ ms.

Closed time distribution

The observed closed times range from 0.15 ms to 10 s in duration (Fig. 5 *A*). The distribution has several small shoulders, although they are not marked. On a log–log scale, the slope of the distribution is −1.55 (correlation coefficient $r = -0.997$).

At least $N_c = 6$ closed states are required to fit an M model to the data (McGee et al., 1988). The time constants of the PDF (Table 4) are relatively close together, especially for the faster components, which is consistent with the absence of pronounced shoulders on the distribution. The value of $P_{obs} = 0.509$ shows that ~50% of the closings are briefer than t_{min}. This is partially a result of adopting a high value of t_{min} during data reduction. This was necessary given the low (18 pS) conductance of the channel.

Tables 3 and 4 show that the only other models giving satisfactory fits to the K^+ channel data are F and D_1. The resultant fits are shown alongside the M model fit in Fig. 5 *A*. All three models account for the whole range of closed times. The cumulative error plots (Fig. 5 *B*) suggest a model ranking M > D_1 > F, which is consistent with that based on the *SC* values (Table 4).

The F fit requires more detailed examination. The fractal dimension is very close to the upper limit

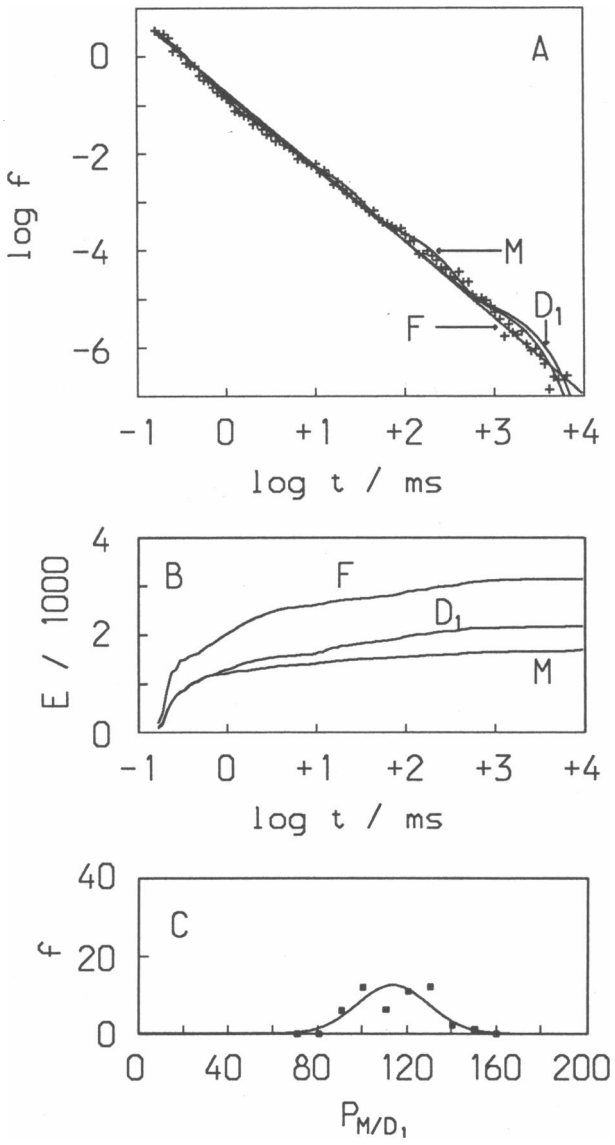

FIGURE 5 Closed time distribution for K^+ channel. (*A*) Observed distribution and PDFs for M, F, and D_1 models (see Table 4). (*B*) The corresponding cumulative error curves. (*C*) *SC* predictor distribution for comparison of M and D_1 models.

TABLE 4 K^+ channel closed time PDFs

Model	Parameters		*SC*	Rank	P_{obs}
M	$\alpha_1 = 0.568$ $\alpha_2 = 0.226$ $\alpha_3 = 0.101$ $\alpha_4 = 0.067$ $\alpha_5 = 0.029$ $\alpha_6 = 0.008$	$\tau_1 = 0.122$ ms $\tau_2 = 0.347$ ms $\tau_3 = 1.86$ ms $\tau_4 = 12.0$ ms $\tau_5 = 116$ ms $\tau_6 = 1210$ms	2.151×10^4	1	0.509
F	$A = 0.543$ ms^{D-1}	$D = 1.985$	2.178×10^4	3	1.06×10^{-15}
D_1	$\beta = 6.22$ ms^{-1}	$\lambda = 2.81$ ms^{-1}	2.156×10^4	2	0.535
D_3	$\beta = 2.35$ ms^{-1}	$\lambda = 0.0843$ ms^{-1}	2.321×10^4	4	0.711
W	$\tau = 1.20 \times 10^{-6}$ ms	$\beta = 0.152$	2.413×10^4	5	0.543
E	$A = 0.300$ ms^{-1}	$D = 0.0290$ ms^{-1}	3.936×10^4	6	0.956

($D = 1.985$). One result of this is that numerous brief closings are predicted, giving $P_{obs} = 1.06 \times 10^{-15}$. This is somewhat unrealistic, as it is easy to show (e.g., by simulation) that the response time of the patch clamp amplifier would reduce such brief closings to a "blur" of noise which would be readily detected at the experimental level. Inspection of the original single channel recordings (see, e.g., Fig. 2 of McGee et al., 1988) shows this not to be the case. On the basis of this, plus the cumulative error plot (Fig. 5 *B*) the F model is excluded from further consideration.

The D_1 model provides a somewhat better description of the data. The model parameters (Table 4) are such that $\beta \approx \lambda$, i.e., there are approximately equal probabilities of the channel reopening or of diffusing among the array of closed states just after the channel has closed. Millhauser et al. (1988*a*) predicted that under such conditions the PDF would be approximated to by a $t^{-3/2}$ power function, which is consistent with the log–log slope of the observed distribution (see above). The bootstrap procedure is therefore of some importance in distinguishing between the M and D_1 models. This yielded a mean predictor value of $\bar{P}_{M/D_1} = 114$, corresponding to a probability of $1 - 5.2 \times 10^{-13}$. Note that the D_1 fit corresponds to $N_c = 100$ closed states. A corresponding fit with $N_c = 50$ states was almost identical. It therefore seems unlikely that increasing the number of closed states to e.g., 200 would yield a significantly better fit, although we have not explored this in detail. Thus, the M model appears to provide the best description of the K^+ channel closed time data.

Open time distribution

The open time distribution is shown in Fig. 6 *A*. There is a clear excess, over a single exponential, of brief openings, and also a small shoulder at ~100 ms. The openings range from 0.15 to something over 100 ms in duration.

The M model fit to the data confirms the earlier analysis of McGee et al. (1988) in requiring $N_o = 3$ components. The fit is excellent, both for the long and for short openings. Model F (Table 5) yielded an adequate fit to the data, with fractal dimension $D = 1.34$ (cf. $D = 1.28$ for qGluR open times), but did not reproduce the shoulders on the observed distribution. Models D_1, W, and E gave poor fits to the data. The most convincing alternative to the M model was the D_3 model, the fit of which is shown in Fig. 6 *A*. The D_3 fit reproduces the excess of brief openings, but does not fully account for the long openings, as can be seen by inspection of the cumulative error plot (Fig. 6 *B*). The parameter values (Table 5) are such that $\beta \approx \lambda$. Interestingly, this differs from the two fits obtained by Lauger (1988), for nicotinic acetylcholine receptor and for K^+ channel closed times, in both of which cases $\beta/\lambda \approx 30$. Application of the bootstrap analysis (Fig. 6 *C*) gives $P_{M/D_3} = 187$, corresponding to a probability of $1 - 2.7 \times 10^{-19}$. It would therefore seem reasonable to conclude that the M model gives the best fit to the data.

Overall ranking of models

The fits given by the six models to the four dwell time distributions were all analyzed by the bootstrap procedure to yield distributions of the *SC* predictors, the means and standard deviations of which are given in Table 3. The standard deviations provide a measure of the extent to which the predictor value is dependent on the dataset sampling errors. The mean predictor values were used to rank the six models for each dataset. The resultant model rankings are listed in Table 6. The only consistent pattern that emerges is that the highest rank is always given to the M model. The second rank position is shared between the F, W, D_1, and D_3 models. So we conclude that the gating kinetics of both channels are best described by the standard M models.

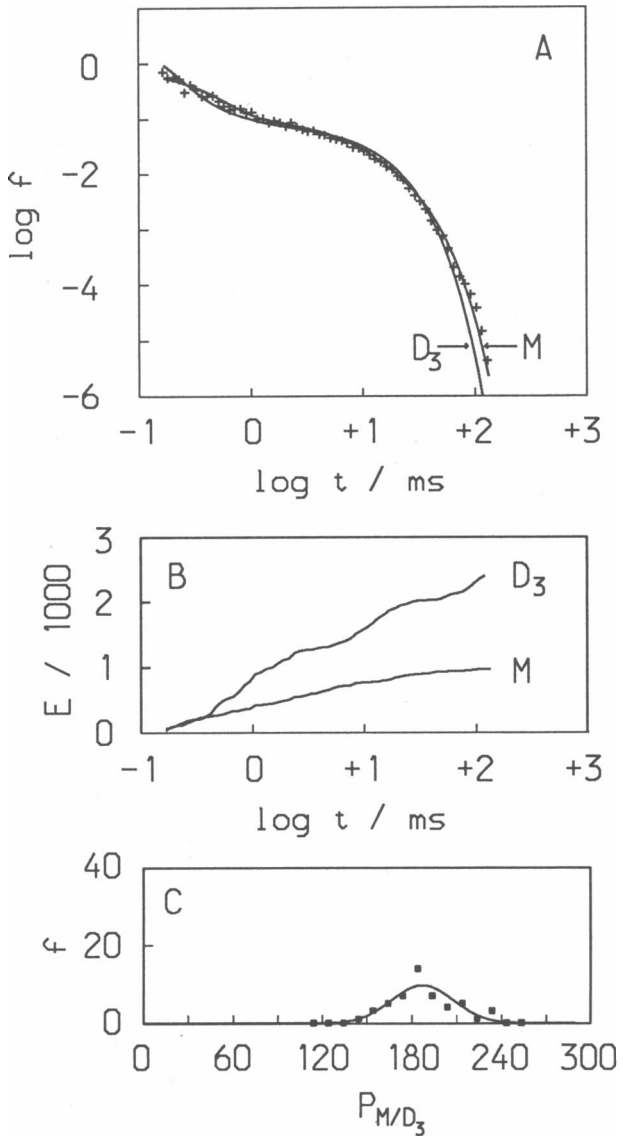

FIGURE 6 Open time distribution for K^+ channel. (*A*) PDFs fitted for M and D_3 models compared with the observed distribution. (*B*) Cumulative error curves for the two fits. (*C*) Distribution of *SC* predictor P_{M/D_3}.

DISCUSSION

In general terms, there are two types of models that may be used to interpret the gating kinetics of ion channels (Fig. 7). The Markov (M) model, dating back to Hodgkin and Huxley (1952) and to Fitzhugh (1965), attempts to explain channel gating kinetics in terms of transitions between a small number of discrete conformational states. As such, it is analogous to, for example, the use of models involving discrete conformational states to account for the allosteric properties of enzymes and other proteins (Monod et al., 1965).

Other models, the "not M" models (Fig. 7), are consistent with the existence of a large number of conformational substates of similar energy. The F, D, W, and E models discussed in this paper fall into this class. Although the initial definition of the F model (Liebovitch et al., 1987*a*) may appear to be something of an algebraic convenience, Liebovitch (1989*a*) has recently pointed out the relationship of this class of models to D-type models. Fractal models of the dynamics of condensed matter systems have been discussed in more general terms by Shlesinger (1988). Lauger (1988) has suggested that the multiple closed states of D models may represent migration of a side-chain packing defect through the channel protein molecule. Although the W model is more empirically based, Klafter and Blumen (1985), for example, have pointed out that a variety of microscopic mechanisms, including defect diffusion, may underly the observed kinetics. It has been stated that evidence supporting a large number of conformational substates comes from a variety of studies on protein molecules. Although this is true, to argue that this implies that channel gating kinetics will reveal such substates is to take an oversimplistic a view of protein dynamics. In their recent review, Frauenfelder et al. (1988) point out that proteins should be viewed as existing in distinct conformational states, each of which gives rise to a hierarchy of conformational substates (CSs). At physiological temperatures, the CSs would be expected to interconvert rapidly, and so would be unlikely to be detectable on the time scale of channel gating kinetics. For instance, one reason for supposing the existence of CSs is the observation of nonexponential ligand rebinding kinetics after, e.g., photodissociation of carbon monoxide from myoglobin. However, such nonexponential ligand binding kinetics are generally measured at low temperatures (160°K and below). At 300°K, nonexponential relaxation might only be expected on a time scale of 100 ps or less. It would seem, therefore, that one cannot provide conclusive support for not-M models of channel gating on the basis of studies of protein dynamics. One must resort, therefore, to statistical analysis of experimental channel data.

By such statistical analysis we have provided support for the M model of channel gating. A similar conclusion has been reached by Korn and Horn (1988) and by McManus et al. (1988), both of whom compared M and F models. Therefore, independent analyses of dwell time distributions for at least seven different ion channel species have provided support for M models. This conclusion is supported by several studies of correlations between successive channel dwell times (Ashford, et al., 1984; Labarca et al., 1985; McManus et al., 1985; Kerry et al., 1987, 1988; Ball et al., 1988; Blatz and Magleby,

TABLE 5 K^+ channel open time PDFs

Model	Parameters		SC	Rank	P_{obs}
M	$\alpha_1 = 0.214$ $\alpha_2 = 0.320$ $\alpha_3 = 0.466$	$\tau_1 = 0.302$ ms $\tau_2 = 5.02$ ms $\tau_3 = 13.7$ ms	4.325×10^4	1	0.903
F	$A = 0.197$ ms^{D-1}	$D = 1.34$	4.347×10^4	2	0.919
D_1	$\beta = 0.116$ ms^{-1}	$\lambda = 0.00112$ ms^{-1}	4.483×10^4	5	0.978
D_3	$\beta = 4.25$ ms^{-1}	$\lambda = 1.68$ ms^{-1}	4.347×10^4	2	0.703
W	$\tau = 0.917$ ms	$\beta = 0.451$	4.366×10^4	3	0.951
E	$A = 0.164$ ms^{-1}	$D = 0.0522$ ms^{-1}	4.417×10^4	4	0.933

1989). This phenomenon is readily explained in terms of M models with multiple-gateway states (Fredkin et al., 1985; Colquhoun and Hawkes, 1987; Ball and Sansom, 1988*b*). By using a semi-Markov framework (Cinlar, 1969), the other models considered could be modified to contain multiple-gateway states in order to explain such correlations. Furthermore, the diffusion models could be modified so that, e.g., the closed-closed transition rates were not all exactly equal. Although this might improve the fit of such models to the data, it would tend to blur the distinction between diffusion models and "classical" Markov models.

In fitting the PDFs for the different models to the observed distributions, we have only made a preliminary correction for the effect of omission of brief openings and closings. To make a more rigourous correction, it would be necessary to extend the theory of event omission that has been worked out for M models (Roux and Sauvé, 1985; Blatz and Magleby, 1986*b*; Ball and Sansom, 1988*a*) to the other classes of models. This could be done using the theoretical framework described by Milne et al (1988).

Overall, both our analysis and that of other workers in the field (Horn and Korn 1989; McManus et al., 1989) support the continued use of M models to interpret channel gating kinetics. This is of some importance, inasmuch as powerful methods of fitting M models to experimental data have been developed Horn and Lange, 1983; Ball and Sansom, 1989). The stage has been reached at which analysis of channel data in terms of M models is beginning to provide important information concerning the molecular events controlling channel gat-

TABLE 6 Summary of model rankings

Dataset	Model ranking
GluR, closed times	M > F > W > D_1 > E > D_3
GluR, open times	M > W > E > F > D_1 > D_3
K^+ channel, closed times	M > D_1 > F > W > D_3 > E
K^+ channel, open times	M > D_3 > F > W > E > D_1

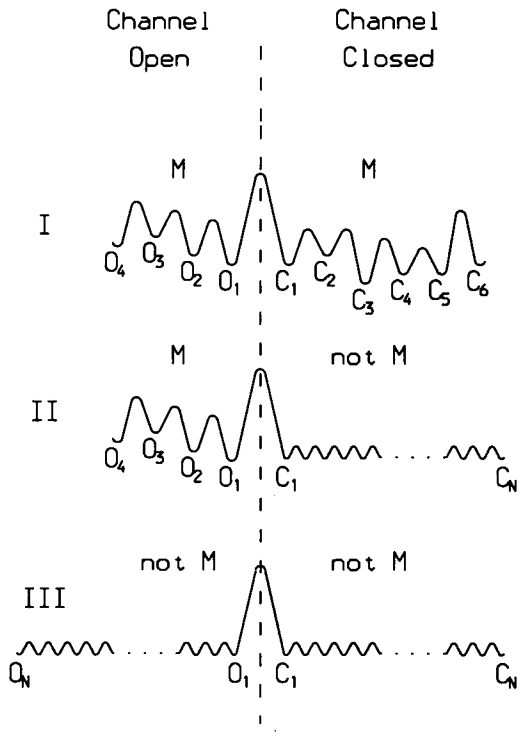

FIGURE 7 Diagram illustrating the difference between M and "not M" gating models. The peaks and troughs represent the energy profile of the channel, for both the open (*left*) and closed (*right*) states. In the M models, the relatively small number of channel states (troughs) are of different energy levels and are separated by relatively high activation energies (peaks). In the not-M models there are many energetically equivalent substates, with low activation energies separating them for one another. It has been assumed that there is a single, open gateway state and a single, closed gateway state, and that the activation energy barrier separating them is relatively high. Three situations are illustrated. (I) Both the open and closed states are described by M models; (II) only the open states are described by an M model; and (III) both the open and closed states are described by not-M models.

ing, e.g., the pharmacology of receptor-channel activation by different agonists (Papke et al., 1988; Ogden et al., 1987). Answering questions about the conformational substates of channel proteins, however, may require the development of more subtle probes than those provided by single-channel recording.

APPENDIX 1

Derivation of the transition matrix for the D_1 gating model

The transition probability rates for a channel gating model may be summarized in a transition rate (Q) matrix, as described by, e.g., Colquhoun and Hawkes (1981, 1982). This is an $N \times N$ matrix, where N is the total number of channel states, where q_{ij} $i \neq j$ is the transition rate for step $i \rightarrow j$, and $q_{ii} = -\Sigma_{i \neq j} q_{ij}$, i.e., the leading diagonal gives the decay rates of the channel states. The Q matrix may be partitioned into submatrices

$$Q = \begin{bmatrix} Q_{oo} Q_{oc} \\ Q_{co} Q_{cc} \end{bmatrix} \tag{A1}$$

such that Q_{cc} describes the closed-state to closed-state transitions, etc. This partitioned form of the Q matrix may then be used to (numerically) evaluate the α_i's and τ_i's of the dwell time PDFs (see, e.g., Colquhoun and Hawkes, 1981, for details).

The D_1 gating model can readily be expressed in terms of the relevant Q matrix. If, for example, we consider the gating mechanism:

$$O \underset{}{\overset{\beta}{\longleftarrow}} C_1 \underset{\lambda}{\overset{\lambda}{\rightleftharpoons}} C_2 \underset{\lambda}{\overset{\lambda}{\rightleftharpoons}} \cdots\cdots \underset{\lambda}{\overset{\lambda}{\rightleftharpoons}} C_{N_C-1} \underset{\lambda}{\overset{\lambda}{\rightleftharpoons}} C_{N_C},$$

where the closed states are numbered $C_1 = 1$ to $C_{N_c} = N_c$, then the rules for generating Q_{cc} (where $(Q_{cc})_{i,j}$ is here the i,jth element of Q_{cc}) are:

$$\begin{aligned} (Q_{cc})_{1,1} &= -(\beta + \lambda) \\ (Q_{cc})_{i,j} &= -2\lambda \qquad i = 2, \ldots, N_c \\ (Q_{cc})_{i,i+1} &= \lambda \qquad i = 1, \ldots, N_c - 1 \\ (Q_{cc})_{i-1,i} &= \lambda \qquad i = 2, \ldots, N_c \end{aligned} \tag{A2}$$

with all other elements of Q_{cc} set to zero. Once Q_{cc} has been generated, the corresponding PDF can be evaluated using the standard methods.

APPENDIX 2

Derivation of the transition matrix for the D_3 gating model

Here we deal with the derivation of the Q_{cc} matrix for a $3 \times 3 \times 3$ D_3 gating model. Extension to the $5 \times 5 \times 5$ and higher-order models is straightforward.

The simplest way to generate the Q_{cc} matrix for the mechanism illustrated in Fig. 1 is to devise a set of rules comparable to those in Eq. A2, yielding a 27×27 matrix. However, by consideration of the symmetry properties of the gating mechanism (Fig. 8), one can arrive at a simpler 9×9 Q_{cc} matrix. This saves on subsequent computing time.

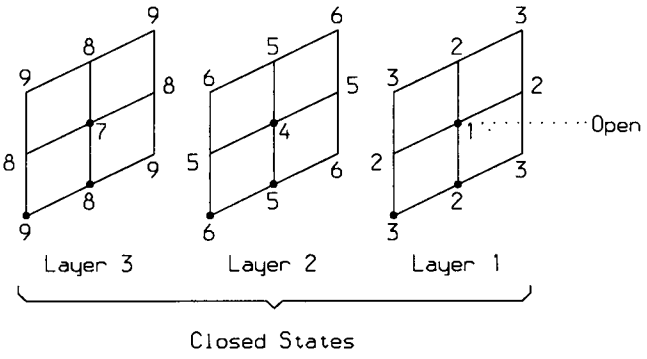

FIGURE 8 Diagram of the nine types of closed state derived from the $3 \times 3 \times 3$ D_3 gating model by symmetry considerations. Thus there is one each of type 1, type 4, and type 7 states, and there are four each of types 2, 3, 5, 6, 8, and 9. So, for example, there are four ways in which the channel can move from a type 1 state to a type 2 state but, once the channel occupies a type 2 state, there is only one way in which it may move back to a type 1 state. Hence, $(Q_{cc})_{1,2} = 4\lambda$ but $(Q_{cc})_{2,1} = \lambda$ (see Eq. A3).

The Q_{cc} matrix that thus arrived at is:

$$Q_{cc} = \lambda \begin{bmatrix} -(5+\beta) & 4 & 0 & 1 & 0 & 0 & 0 & 0 & 0 \\ 1 & -4 & 2 & 0 & 1 & 0 & 0 & 0 & 0 \\ 0 & 2 & -3 & 0 & 0 & 1 & 0 & 0 & 0 \\ 1 & 0 & 0 & -6 & 4 & 0 & 1 & 0 & 0 \\ 0 & 1 & 0 & 1 & -5 & 2 & 0 & 1 & 0 \\ 0 & 0 & 1 & 0 & 2 & -4 & 0 & 0 & 1 \\ 0 & 0 & 0 & 1 & 0 & 0 & -5 & 4 & 0 \\ 0 & 0 & 0 & 0 & 1 & 0 & 1 & -4 & 2 \\ 0 & 0 & 0 & 0 & 0 & 1 & 0 & 2 & -3 \end{bmatrix} \tag{A3}$$

The corresponding PDF is then generated by the standard methods.

This work was supported by grants from the UK SERC (to Drs. Sansom, Ramsey, and Usherwood) and the Wellcome Trust (to Dr. Sansom).

Received for publication 16 May 1989 and in final form 31 July 1989.

REFERENCES

Akaike, H. 1974. A new look at the statistical model identification. *IEEE (Inst. Electr. Electron. Eng.) Trans. Autom. Control.* AC19:716-723.

Ashford, M. L. J., C. J. Kerry, K. S. Kits, R. L. Ramsey, M. S. P. Sansom, and P. N. R. Usherwood, 1984. Kinetic analysis of channels gated by L-glutamate receptors in locust muscle membrane. *In* Biophysics of Membrane Transport. B. Tomicki, J. J. Kuczera, and S. Prezstalski, editors. University of Wroclaw Press, Wroclaw. 157–166.

Ball, F. G., C. J. Kerry, R. L. Ramsey, M. S. P. Sansom, and P. N. R. Usherwood. 1988. The use of dwell time cross-correlation functions to study single ion channel gating kinetics. *Biophys. J.* 54:309–320.

Ball, F. G., and M. S. P. Sansom. 1988*a*. Aggregated Markov processes incorporating time interval omission. *Adv. Appl. Prob.* 20:546–572.

Ball, F. G., and M. S. P. Sansom, 1988*b*. Single channel autocorrelation functions: the effects of time interval omission. *Biophys. J.* 53:819–832.

Ball, F. G., and M. S. P. Sansom. 1989. Single channel gating mechanisms model identification and parameter estimation. *Proc. R. Soc. Lond. B Biol. Sci.* 236:385–416.

Ball, F. G., M. S. P. Sansom, and P. N. R. Usherwood. 1989. A comparison of different gating models for voltage- and receptor-gated ion channels. *J. Physiol. (Lond.)*. In press. (Abstr.)

Blatz, A. L., and K. L. Magleby. 1986*a*. Quantitative description of three modes of activity of fast chloride channels from rat skeletal muscle. *J. Physiol. (Lond.)*. 378:141–174.

Blatz, A. L., and K. L. Magleby. 1986*b*. Correcting single channel data for missed events. *Biophys. J.* 49:967–980.

Blatz, A. L., and K. L. Magleby. 1989. Adjacent interval analysis distinguishes among gating mechanisms for the fast chloride channel from rat skeletal muscle. *J. Physiol. (Lond.)*. 410:561–585.

Cinlar, E. 1969. Markov renewal theory. *Adv. Appl. Prob.* 1:123–187.

Colquhoun, D., and A. G. Hawkes. 1981. On the stochastic properties of single ion channels. *Proc. R. Soc. Lond. B Biol. Sci.* 211:205–235.

Colquhoun, D., and A. G. Hawkes. 1982. On the stochastic properties of bursts of single ion channel openings and of clusters of bursts. *Philos. Trans. R. Soc. Lond. B Biol. Sci.* 300:1–59.

Colquhoun, D., and A. G. Hawkes. 1987. A note on correlations in single ion channel records. *Proc. R. Soc. Lond. B Biol. Sci.* 230:15–52.

Colquhoun, D., and F. J. Sigworth. 1983. Fitting and statistical analysis of single-channel records. *In* Single-Channel Recording. B. Sakmann and E. Neher, editors. Plenum Publishing Corp., New York. 191–263.

Cox, D. R., and H. D. Miller. 1965. The Theory of Stochastic Processes. Methuen, London. 398 pp.

Easton, D. M. 1978. Exponentiated exponential model (Gompertz kinetics) of Na^+ and K^+ conductance changes in squid giant axon. *Biophys. J.* 22:15–28.

Efron, B. 1981. Nonparametric standard errors and confidence intervals. *Can. J. Stat.* 9:139–172.

Efron, B. 1982. The Jackknife, the Bootstrap and Other Resampling Plans. Society of Industrial and Applied Mathematics, Philadelphia.

Fitzhugh, R. 1965. A kinetic model of the conductance changes in nerve membrane. *J. Cell. Comp. Physiol.* 66:111–118.

Frauenfelder, H., F. Parak, and R. D. Young. 1988. Conformational substates in proteins. *Annu. Rev. Biophys. Biophys. Chem.* 17:451–79.

Fredkin, D. R., M. Montal, and J. A. Rice. 1985. Identification of aggregated Markovian models: application to the nicotinic acetylcholine receptor. *In* Proceedings of the Berkeley Conference in Honor of Jerzy Neyman and Jack Kiefer. L. M. Le Cam and R. A. Ohlsen, editors. Wadsworth Publishing Co., Belmont, CA. 269–289.

French, A. S., and L. L. Stockbridge. 1988. Fractal and Markov behaviour in ion channel kinetics. *Can. J. Physiol. Pharmacol.* 66:967–970.

Hamill, O. P., A. Marty, E. Neher, B. Sakmann, and F. J. Sigworth. 1981. Improved patch-clamp techniques for high-resolution current recording from cells and cell-free membrane patches. *Pflügers Arch. Eur. J. Physiol.* 391:85–100.

Hodgkin, A. L., and A. F. Huxley. 1952. A quantitative description of membrane current and its application to conduction and excitation in nerve. *J. Physiol. (Lond.)*. 117:500-544.

Horn, R. 1984. Gating of channels in nerve and muscle: a stochastic approach. *In* Ion Channels: Molecular and Physiological Aspects. W. D. Stein, editor. Academic Press, Inc., New York. 53–97.

Horn, R. 1987. Statistical methods for model discrimination: applications to gating kinetics and permeation of the acetylcholine receptor channel. *Biophys. J.* 51:255–263.

Horn, R., and S. J. Korn. 1989. Model selection: reliability and bias. *Biophys. J.* 55:379–381.

Horn, R., and K. Lange. 1983. Estimating kinetic constants from single channel data. *Biophys. J.* 43:207–233.

Kerry, C. J., K. S. Kits, R. L. Ramsey, M. S. P. Sansom, and P. N. R. Usherwood. 1987. Single channel kinetics of a glutamate receptor. *Biophys. J.* 51:137–144.

Kerry, C. J., R. L. Ramsey, M. S. P. Sansom, and P. N. R. Usherwood. 1988. Glutamate receptor-channel kinetics: the effect of glutamate concentration. *Biophys. J.* 53:39–52.

Klafter, J., and A. Blumen. 1985. Models for dynamically controlled relaxation. *Chem. Phys. Lett.* 119:377–382.

Klafter, J., and M. F. Shlesinger. 1986. On the relationship among three theories of relaxation in disordered systems. *Proc. Natl. Acad. Sci. USA.* 83:848–851.

Korn, S. J., and R. Horn. 1988. Statistical discrimination of fractal and Markov models of single-channel gating. *Biophys. J.* 54:871–877.

Labarca, P., J. A. Rice, D. R. Fredkin, and M. Montal. 1985. Kinetic analysis of channel gating: application to the cholinergic receptor channel and the chloride channel from *Torpedo californica*. *Biophys. J.* 47:469–478.

Landaw, E. M., and J. J. DiStefano. 1984. Multiexponential, multicompartmental, and noncompartmental modelling. II. Data analysis and statistical considerations. *Am. J. Physiol.* 246:R665–R677.

Lauger, P. 1988. Internal motions in proteins and gating kinetics of ionic channels. *Biophys. J.* 53:877–884.

Liebovitch, L. S. 1989*a*. Analysis of fractal ion channel gating kinetics: kinetic rates, energy levels and activation energies. *Math. Biosci.* 93:97–115.

Liebovitch, L. S. 1989*b*. Testing fractal and Markov models of ion channel kinetics. *Biophys. J.* 55:373–377.

Liebovitch, L. S., J. Fischbarg, and J. P. Koniarek. 1987*a*. Ion channel kinetics: a model based on fractal scaling rather than multistate Markov processes. *Math. Biosci.* 84:37–68.

Liebovitch, L. S., J. Fischbarg, J. P. Koniarek, I. Todorova, and M. Wang. 1987*b*. Fractal model of ion-channel kinetics. *Biochim. Biophys. Acta.* 896:173–180.

Liebovitch, L. S., and J. M. Sullivan. 1987. Fractal analysis of a voltage-dependent potassium channel from cultured mouse hippocampal neurones. *Biophys. J.* 52:979–988.

McGee, R., M. S. P. Sansom, and P. N. R. Usherwood. 1988. Characterization of a delayed rectifier K^+ channel in NG108-15 neuroblastoma × glioma cells: changes in gating kinetics associated with the enrichment of membrane phospholipids with arachidonic acid. *J. Membr. Biol.* 102:21–34.

McManus, O. B., A. L. Blatz, and K. L. Magleby. 1985. Inverse relationship of the durations of adjacent open and shut intervals for Cl and K channels. *Nature (Lond.)*. 317:625–627.

McManus, O. B., A. L. Blatz, and K. L. Magleby. 1987. Sampling, log binning, fitting, and plotting durations of open and shut intervals from single ion channels and the effects of noise. *Pflügers Arch. Eur. J. Physiol.* 410:530–553.

McManus, O. B., and K. L. Magleby. 1988. Kinetic states and modes of single large-conductance Ca-activated K channels in cultured rat skeletal muscle. *J. Physiol. (Lond.)*. 402:79–120.

McManus, O. B., C. E. Spivak, A. L. Blatz, D. S. Weiss, and K. L. Magleby. 1989. Fractal models, Markov models, and channel kinetics. *Biophys. J.* 55:383–385.

McManus, O. B., D. S. Weiss, C. E. Spivak, A. L. Blatz, and K. L. Magleby. 1988. Fractal models are inadequate for the kinetics of four different ion channels. *Biophys. J.* 54:859–870.

Millhauser, G. L., E. E. Salpeter, and R. E. Oswald. 1988*a*. Diffusion models of ion-channel gating and the origin of power-law distributions from single-channel recording. *Proc. Natl. Acad. Sci. USA*. 85:1502–1507.

Millhauser, G. L., E. E. Salpeter, and R. E. Oswald. 1988*b*. Rate-amplitude correlation from single-channel records: a hidden structure in ion channel gating kinetics? *Biophys. J.* 54:1165–1168.

Milne, R. K., G. F. Yeo, R. O. Edeson, and B. W. Madsen. 1988. Stochastic modelling of a single ion channel: an alternating renewal approach with application to limited time resolution. *Proc. R. Soc. Lond. B Biol. Sci.* 233:247–292.

Monod, J. J. Wyman, and J. P. Changeux. 1965. On the nature of allosteric transitions: a plausible model. *J. Mol. Biol.* 12:88–118.

Ogden, D. C., D. Colquhoun, and C. G. Marshall. 1987. Activation of nicotinic ion channels by acetylcholine analogues. *In* Cellular and Molecular Basis of Cholinergic Function. M. J. Dowdall and J. N. Hawthorne, editors. Ellis Horwood, Chichester, UK. 133–151.

Papke, R. L., G. Millhauser, Z. Lieberman, and R. E. Oswald. 1988. Relationships of agonist properties to the single channel kinetics of nicotinic acetylcholine receptors. *Biophys. J.* 53:1–10.

Roux, B., and R. Sauvé. 1985. A general solution to the time interval omission problem applied to single channel analysis. *Biophys. J.* 48:149–158.

Schwarz, G. 1978. Estimating the dimension of a model. *Ann. Stat.* 6:461–464.

Shlesinger, M. F. 1988. Fractal time in condensed matter. *Annu. Rev. Phys. Chem.* 39:269–290.

Shlesinger, M. F., and E. W. Montroll. 1984. On the Williams-Watts function of dielectric relaxation. *Proc. Natl. Acad. Sci. USA*. 81:1280–1283.